[Frontiers in Bioscience 11, 3036 -3048, September 1, 2006]

Mechanisms of doxycycline-induced cytotoxicity on human bronchial epithelial cells

Matthieu Sourdeval [1], Christophe Lemaire [2], Catherine Brenner [2], Emmanuelle Boisvieux-Ulrich [1] and Francelyne Marano [1]

[1] Laboratoire de Cytophysiologie et Toxicologie Cellulaire, Université Paris 7 Denis Diderot, 2 Place Jussieu, 75251 Paris Cedex 05, France ; [2] Laboratoire de Génétique et Biologie Cellulaire, Université de Versailles/St Quentin, CNRS FRE 2445, 45 av. des Etats-Unis, 78 035 Versailles Cedex, France

TABLE OF CONTENT

1. ABSTRACT

Doxycycline (DOX), a synthetic tetracycline, may have potential utility in the management of cancers and in the treatment of chronic inflammatory diseases due to its role in growth, invasion and metastasis of many tumors, on cell proliferation and as inducer of apoptosis. Some studies established its role in the treatment of lesions induced by mustards, warfare agents causing severe damage with blistering and tissue detachment in exposed areas of the body. In the present study, the effect of Dox was investigated in a human bronchial epithelial cell line. Dox induced a time- and concentration-dependent cell proliferation inhibition, associated with a cell cycle arrest in S phase, a decrease in viability due to apoptosis and necrosis, and cell detachment. This latter was partly correlated with early activation of caspase-3 before detachment, and with mitochondrial alteration. Cell transfection with a Bcl-2 encoding vector showed a decrease both in mitochondrial depolarization and cell detachment. Dox-induced apoptosis included decrease in Bcl-2 expression, increase in Bak expression and caspase-3 and –9 activation but appeared to be p53- and Bax-independent. A better comprehension of the Dox-induced apoptotic pathway could allow to abolish its toxic effects, improving the therapeutic efficiency of Dox.

2. INTRODUCTION

Doxycycline (DOX), a synthetic tetracycline have been used to threat several localized inflammatory diseases, such as chronic acne, periodontis, rosacea (1-3). Nevertheless, even if Dox has effectively been shown to be well tolerated in numerous human models, both *in vitro* (4-6) and *in vivo* (3, 7), the recommended conditions of use largely vary according to the model considered. Moreover, emerging studies reveal its toxicity even in normal cell line (8-11) or *in vivo* (12). This toxicity may have potential utility in the management of cancers in regard to its effect on growth, cell proliferation and apoptosis (7, 13). Apoptosis, a programmed cell death notably involved in development and tissue homeostasis, is triggered by receptor-mediated (extrinsic) or mitochondria-related (intrinsic) signaling pathways. Activation of the intrinsic pathway requires mitochondrial membrane permeabilization (MMP) and release of pro-apoptotic mitochondrial proteins normally found in the intermembrane space. Such proteins include both molecules involved in the activation of caspases (e.g. cytochrome c) (14, 15) and molecules involved in caspase-independent cell death (e.g. Apoptosis Inducing Factor (AIF) and endonuclease G (EndoG) (16)). The MMP can be achieved by the opening of the permeability transition pore complex (PTPC), a large proteinaceous complex, which is regulated by members of the Bcl-2 family (17).

A better comprehension of the toxic effects induced by Dox and of their mechanisms could allow the possibility to decrease the dramatic side effects associated with Dox treatment and to optimize the Dox therapeutic potential of cancer cells (7). To date, only a few specific studies have been performed on respiratory epithelial cell models. However, respiratory system is a primary target of diseases such as mycoplasma pneumoniae (18), a parasite of the human respiratory tract inducing atypic pneumonia, or as obstructive chronic bronchopneumopathia or of biological or chemical warfare exposure such as anthrax (19, 20) or sulfur mustard (21), both of them cared *in vivo* by Dox treatment.

In this study, we determined the early mechanisms of toxicity induced by Dox in the 16HBE human bronchial epithelial cell line, which is a cell line both representative of the upper airway respiratory tract, a primary target of diseases or warfare agents' lesions cared by Dox treatment and a good model for toxicity studies, notably for apoptotic mechanisms (22). Our experiments showed that Dox induced a series of toxic effects, such as inhibition of proliferation, cell cycle arrest, cell detachment and apoptosis, all of them time- and concentration-dependent. These results demonstrated that Dox triggers an apoptosis specifically mediated by the mitochondrial pathway and notably via the interplay of the mitochondrial-related proteins Bcl-2 and Bak and via the caspase-3 and -9 activation.

3. MATERIALS and METHODS

3.1. Cell culture

The 16HBE14o- cell line was a generous gift of Dr. Gruenert (N.I.H., San Francisco, CA, USA) and was originally isolated from human bronchial epithelial cells transformed by the origin-defective simian virus SV40 (23). Cells were grown in DMEM/ Ham F12 culture medium (Gibco, Cergy-Pontoise, France) supplemented with 2% Ultroser G, 1% glutamine, 0.5% fungizone and antibiotics (100 U/mL penicillin, 100 µg/mL streptomycin) (Invitrogen, Cergy Pontoise, France). Cells were seeded at 30 000 cells/cm² in 6-, 12- or 96 well plates coated with type I collagen and incubated at 37°C in a humidified atmosphere of 5% CO2. Cells were used during the exponential growth phase and the cell line doubling time was approximately 24 h.

3.2. Chemical treatment

48 h after seeding, subconfluent monolayers were washed with DMEM/ Ham F12 without Ultroser G and treatments were carried out in DMEM/ Ham F12 without Ultroser G. Dox (Dox) was purchased from Sigma Chemical Co. (St Louis, MO, USA). A stock solution (2 mM) was prepared in DMEM/F12 and stored at 4°C for up to one month. Final Dox dilutions were performed immediately before use. Cell cultures were exposed to Dox concentrations ranging from 20 to 100 µM for an exposure time ranging from 30 min to 24 h.

3.3. Dox-induced toxic effects

3.3.1. Cell counts and proliferation

Cells were harvested at different times of treatment. Detached cells were collected in the medium, whereas adherent cells were resuspended in trypsin-EDTA (Invitrogen) solution for 5-10 min at 37°C and inhibited by 10% FCS. Both detached and adherent cell populations were counted using a hemacytometer.

3.3.2. Cell cycle analysis

Briefly, cells were collected, centrifuged and washed in Phosphate Buffered Saline (PBS) buffer. Cells were then fixed in 1 mL cold methanol at –20°C for 1 h, washed once in PBS and resuspended in 1 mL of PBS containing 0.5 % RNase (Sigma). After RNase action, 20 µg/mL of propidium iodide (PI) were added and cells were kept at 4°C until analysis with an EPICS-Elite-ESP flow cytometer (Coultronic, France). Each histogram corresponded to about 10,000 nuclei. Cell nuclei with DNA that had not gone beyond the G1 phase served as an indicator of apoptotic cell death.

3.3.3. BrdU incorporation

Bromodeoxyuridine (BrdU) labelling: cells were grown for 1h in medium supplemented with 20 µM BrdU (Sigma), and washed in BrdU-free medium before treatment with Dox for 24 hours. Cells were washed in PBS and fixed with methanol –20C° after trypsin dissociation, incubated with HCl 0.2N/0.5% Triton X-100 for 15 min to denaturate DNA, and in 0.1 M $Na_2B_4O_7$ to neutralize the acid. BrdU was immunodetected using mouse monoclonal anti-BrdU (Becton Dickinson, Belgique for FACS analysis) and secondary FITC-labelled antibody. Nuclei were counterstained with PI 20 µg/mL in presence of RNase.

3.3.4. WST-1 reduction assay

WST-1 reduction assay (Roche, Mannheim, Germany) is a colorimetric assay for quantification of

cytotoxicity, based on the cleavage of the WST-1 tetrazolium salt by mitochondrial dehydrogenases in viable cells. Before Dox treatment, cells were rinsed twice in DMEM/F12 without HEPES and without red phenol to avoid any interference with WST-1 reduction. The exposure was carried out in the same medium and after 24h exposure, 20 µL of WST-1 reagent (diluted 1:1 in DMEM/F12 without hepes or red phenol) was added to each sample. After 90 min incubation in a humidified atmosphere (37°C, 5% CO2), the optical density of the wells was determined spectrophotometrically at a wavelength of 450 nm with a reference wavelength of 630 nm using a DYNEX MRX microplate reader. A background control (absorbance of culture medium plus WST-1 in the absence of cells) was used as a blank. Results were expressed as a percentage of the WST-1 cleavage in untreated cells (the reference 100% viable cell control). These data are expressed as mean values +/- standard error (SD) (n=8).

3.3.5. Discrimination between live, apoptotic and necrotic cells

In order to determine the type of cell death induced by Dox, detached and adherent cells were incubated for 20 min at 37 °C with fluorescein diacetate (FDA, 1 µg/mL) and ethidium bromide (EtBr, 20 µg/mL) in DMEM/ Ham F12 as described in Lemaire et coll. (24). Cells were immediately observed and counted on a conventional epifluorescence microscope.

3.3.6. Assessment of the involvement of mitochondria in the apoptotic process

The effect of Dox on loss of mitochondrial transmembrane potential ($\Delta\Psi m$) was monitored by measuring the mitochondrial membrane permeabilization (MMP) attributed to early events in apoptosis with a DePsipher kit for mitochondrial membrane potential detection (R&D Systems, UK). Functional mitochondria were assessed by flow cytometry or by *in situ* observation and photographed with a Nikon Optiphot on a conventional epifluorescence microscope (Boisvieux et al., 2005). For kinetics study, treated and untreated cells were harvested, rinsed, resuspended in fresh complete DMEM/F12 medium supplemented with 50 nM 3, 3'-dihexyloxacarbocyanine iodide ($DiOC_6(3)$; Molecular Probes), incubated for 15 min at 37°C, and analyzed by flow cytometry (Elite, Coultronics France). DiOC6(3) is a lipophilic cationic fluorochrome that accumulates in the mitochondrial matrix proportionally to their transmembrane potential (25). Assays were repeated three times and in each case at least 10,000 cells were analyzed.

3.3.7. Western blot analysis

Treated and untreated cells were recovered, rinsed in cold PBS, and lysed in lysis buffer (50 mM HEPES–KOH, pH 7.4, 250 mM NaCl, 1% NP-40, 5 mM EDTA, 0.5 mM DTT and a cocktail of protease inhibitors for 30 min at 4°C. Standardization of protein loading was achieved as follows: (i) protein measurements of all samples were performed using the bicinchoninic acid assay and equal amounts of protein (30 µg per lane) were loaded onto the gel; (ii) transfer efficiency of western blots was routinely checked by staining the membranes with 0.5% Ponceau Red in 1% acetic acid. Proteins were separated by SDS–PAGE (15% acrylamide / 0.2% bisacrylamide for Bax, Bak and Bcl-2 or 10% acrylamide / 0.1% bisacrylamide for p53) and transferred to PVDF nitrocellulose membranes (Millipore, Billerica, Massachusetts, US). Membranes were blocked for 1 h with 5% non-fat dry milk in PBS containing 0.1% Tween-20 and then overnight incubated at 4°C with either anti-Bax (N20, Santa Cruz Biotechnology, California, US), anti-Bak (Santa Cruz), anti-Bcl-2 (Santa Cruz Biotechnology) or anti-p53 ascites antibodies (1:1000). Primary antibodies were labeled with goat anti-mouse IgG at a 1:10,000 dilution or with goat anti-rabbit IgG at a 1:4500 dilution conjugated with horseradish peroxidase (Santa Cruz Biotechnology) for 1 h and proteins were detected using the ECL method according to the manufacturer's instructions (Amersham Biosciences, Buckinghamshire, UK).

3.3.8. Immunofluorescence

For immunostaining, cells were fixed with paraformaldehyde (4% in PBS (wt/vol)), permeabilized by 15 min treatment with Triton X-100 (0.15% final) and stained with mouse monoclonal anti-Bax 6A7 antibody (dilution 1:100; Beckton Dickinson, Erembodegem, Belgium). Cells were then revealed with Alexa fluor 568 goat anti-mouse IgG (dilution 1:100; Invitrogen), or FITC anti-mouse IgG (dilution 1:100; Invitrogen). Nuclei were stained for 5 min with Hoechst 33342 (2 µM; Invitrogen). Cells were then examined under a fluorescence microscope (Leica; DMRBtype).

3.3.9. Cell transfection

16HBE cells were seeded at $1.2x10^5$ cells per well in 12-well plates and transiently cotransfected with 1:4 ratios of GFP encoding vector (p-EGFP-N2, Clonetech) and the vectors of interest (1 µg total DNA per well), respectively. DNA and lipofectamine 2000 reagent (Invitrogen) were mixed according to the manufacturer's recommendations. Wild-type human p53 cDNA was cloned in the pcDNA3.1 vector and then used to create a p53 mutant at codon 175 (histidine instead of arginine) by site-directed mutagenesis (Quickchange, Stratagene). The Bcl-2 encoding vector was previously described (26). Empty plasmid (neo) was used as control. In each experiment, the rate of transfection efficiency was about 35%.

3.3.10. Stably transfected cell lines

HeLa cells, originated from some human cervical cancer cells, stably transfected with empty vector (pcDNA3, neo) or with human *bcl-2* gene (kindly provided by Dr. V. Goldmacher, ImmunoGen, Inc, Cambridge, MA, USA) and HCT116, a cell line originated from some human colon carcinoma, (proficient, $Bax^{-/-}$ or $Bak^{-/-}$; generously provided by B. Vogelstein, The Johns Hopkins University Medical Institutions, Baltimore, MD, USA) were cultured in DMEM/F12 medium supplemented with 10% heat-inactivated FCS and antibiotics (Invitrogen) at 37°C under 5% CO2.

3.3.11. Fluorometric caspases assay

Detection of protease activity (caspase-3 and caspase-8) was determined using the EnzChek Caspase

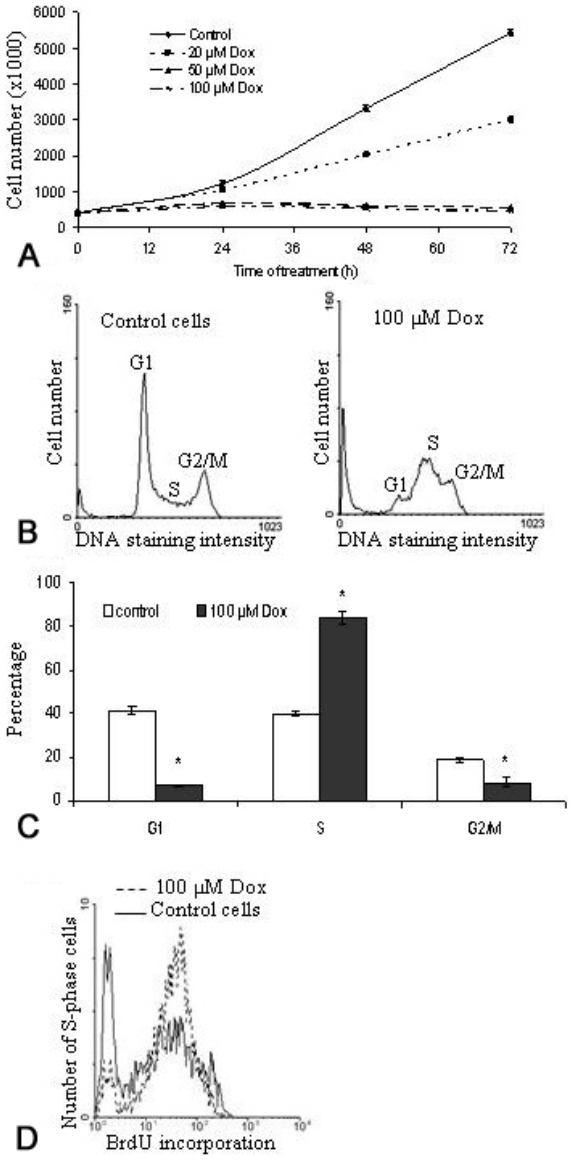

Figure 1. Dox induces proliferation inhibition and cell cyle arrest. A: Proliferation inhibition induced by Dox. B: Cell cycle changes induced by Dox after 24h of treatment. Cells were analyzed by flow cytometry to determine the percentages of sub-G1, G1, S and G2/M fractions. C: Cellquest software analysis of cell distribution in the different phases of the cell cycle. D: Rate of BrdU incorporation in the S-phase cells by immunolabelling of BrdU incorporated after 24h of 100 µM Dox treatment, followed by flow cytometry analysis. Each bar represents means ± SD of 3 separate determinations. * Values significantly different ($p<0.05$) from control.

Assay kit with z-IETD-R 110 as caspase-8 substrate and z-DEVD-R 110 as caspase-3 substrate (Invitrogen). Cells were treated with Dox or left untreated for control, they were harvested and lysed. The lysates were assayed in microplate well with the substrate and the fluorescence was measured (excitation /emission 496/520 nm) using a fluocytometer (Fluostar Galaxy, BMG).

3.3.12. Caspase inhibitors assay

The involvement of caspases was assessed by pre-incubating the cells with cell-permeable irreversible specific caspase inhibitors for 30 min before Dox treatment for 4 or 24 h. Z-VAD-fmk, z-WEHD-fmk, z-VDVAD-fmk, z-DEVD-fmk, z-YVAD-fmk, z-VEID-fmk, z-IETD-fmk, z-LEHD-fmk, z-AEVD-fmk and z-LEED-fmk (Caspase Inhibitor Sample Pack, R&D systems, UK), are respectively a pan caspase, and caspase-1, -2, -3, -4, -6, -8, -9, -10 and -13 inhibitors,. The 20 mM stock solutions in DMSO were stored at –20°C and diluted to 100 µM in medium before use.

3.4. Statistical analysis

All results are representative of at least three separate experiments. Data were analyzed using one-way analysis of variance. Subsequently, the Student-Newman-Keuls test was used for all pairwise comparisons of mean responses among the different treatment groups (SigmaStat). Differences between groups were considered significant if the p value was less than 0.05.
Data are presented as the mean +/- standard error (SD) of the mean for three replicates of one representative experiment.

4. RESULTS

4.1. Dox induces cell proliferation inhibition associated with cell cycle arrest, cell detachment and cell death

4.1.1. Disturbance in cell proliferation

The effect of Dox (20, 50 and 100 µM) on 16HBE cells proliferation was measured 24, 48 and 72h after the beginning of the treatment (Figure 1A). 20µM Dox-treated cultures showed a significant decrease in cell number in comparison with the control after 48h ($2.0x10^6±45.0x10^3$ vs $3.3x10^6±92.0x10^3$) and 72h ($3x10^6±60x10^3$ vs $5.4x10^6±98.0x10^3$) of treatment but not within 24h of treatment ($1.1x10^6±30.0x10^3$ vs $1.2x10^6±88.0x10^3$). In contrast, higher Dox concentrations (50 and 100 µM) resulted in a marked inhibition of proliferation as soon as after 24h of treatment ($684.5x10^3±10.0x10^3$ for 50 µM Dox, $580.2x10^3±27.0x10^3$ for 100 µM Dox vs $1.2x10^6±88.0x10^3$ for the control). After 48 and 72h, the anti-proliferative effect of these high concentrations led to a slight decrease in the cell number in comparison with 24h of treatment, which could result from cellular death or from cell detachment. These results provided evidence of an anti-proliferative effect of Dox on 16HBE cells, depending on time and concentrations of treatment.

4.1.2. Cell cycle arrest

The cell distribution in cell cycle was studied by flow cytometry analysis. Untreated or 100 µM Dox-treated cells were analyzed after DNA staining with propidium iodide and RNase action (Figure 1B), followed by an analysis with the software cellquest (Figure 1C). It appeared that Dox induced significant changes in the cell cycle distribution, with a decrease in G1- and G2/M-phase

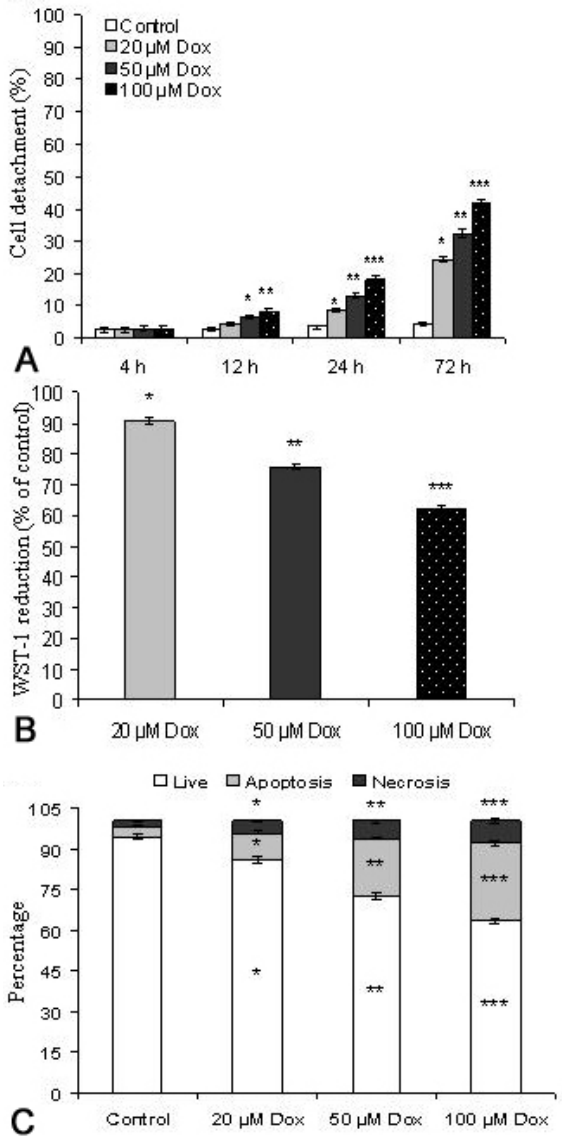

Figure 2. Dox induces cell detachment and cell death. A: Kinetics of cell detachment induced by Dox treatment. B, C: Effect of Dox on cell death. B: WST-1 reduction assay after 24h of Dox treatment. C: Cells were harvested after 24 h treatment and live, apoptotic and necrotic cells were discriminated and counted on an epifluorescence microscope. Data are expressed as percent of cells for each type of death. Each bar represents means ± SD of 3 separate determinations. * Values significantly different ($p<0.05$) from control. Among treatment conditions, values not significantly different have the same number of asterisks.

cells of about 34% and 10% respectively, correlated with a 44% increase of S-phase cells. Such modification in the treated cells distribution in the cell cyle suggested a Dox-induced growth arrest in S-phase. Thus, we examined the rate of BrdU incorporation in the S-phase cells by immunolabelling of BrdU incorporated after 24h of 100 µM Dox treatment, followed by flow cytometry analysis. This clearly showed the increase in number of cells that had incorporated BrdU at the end of Dox-treatment (Figure 1D). Both results indicated that Dox induced the inhibition of proliferation with growth arrest in S-phase and accumulation of cells blocked in S-phase.

4.1.3. Cell detachment

The effects of Dox (20, 50 and 100 µM) on cell detachment were measured with a time-course study by counting cells that remained adherent or became detached after Dox exposure for 4, 12, 24 or 72h (Figure 2A). Dox led to a significant cell detachment process both in a concentration-dependent and a time-dependent manner compared to the control. Cell detachment appeared between 4 and 12 h after the beginning of treatment (8.4±0.8% after 12h in the presence of 100 µM Dox), and increased up to 72 h (41.8±1.0% for 100 µM Dox), whereas the control cultures presented only minor cell detachment (≤ 3%) for each time of analysis. This increase was also concentration-dependent, the cell detachment increasing according to the Dox-treatment concentrations, with 8.6±0.7% and 18.2±1.2% for respectively 20 µM and 100 µM Dox after 24h of treatment.

4.1.4. Cell death

The inhibition of proliferation and the decrease in the cell number at the highest concentrations of Dox could also be explained by induction of cell death process. The quantitative analysis of the DNA content by flow cytometry using propidium iodide revealed that Dox treatment (100 µM) for 24h promoted the formation of a sub-G1 population, with low levels of DNA content characteristic of apoptosis (Figure 1B). The WST-1 assay confirmed this decrease in cell viability in a concentration-dependent manner (Figure 2B). 20µM Dox induced only a slight decrease in cell viability (9.5±1.0%), whereas 100 µM Dox promoted 38.1±1.1% of cell death. To determine the mode of cell death induced by Dox, we used a double staining of unfixed cells with Fluorescein DiAcetate and Etidium Bromide which allowed to easily discriminate between live, apoptotic and necrotic cells. Dox induced a substantial concentration-dependent decrease in the percentage of live cells in comparison with the control (Figure 2D). This decrease was associated with a moderate increase in the percentage of necrotic cells in a concentration-dependent manner, with a maximum of 8.2±0.7% for Dox at 100 µM after 24h treatment in comparison with the 1.9±0.4% occurring in the control cultures. Thus, the decrease in viability induced by Dox was mainly correlated with an apoptotic cell death induction, as revealed by the significant concentration-dependent increase in the number of apoptotic cells after Dox treatment increasing up to 28.5±0.8% after 24h treatment with 100 µM Dox. The control culture exhibited a weak apoptotic rate of 3.6±0.5%.

4.2. Dox induces intrinsic apoptotic pathway

4.2.1. Mitochondrion involvement in Dox-induced apoptosis

Permeabilization of the mitochondrial membrane (MMP) is a critical event of the apoptotic process and is partly controlled by the permeability transition pore

complex (PTPC). We investigated whether exposure to Dox caused MMP and dissipation of the transmembrane potential ΔΨm, by assessing the incorporation of a lipophilic cationic fluorochrome (DePsipher) into mitochondria. Dox-treated and control cells were stained with DePsipher, observed with an epifluorescence microscope and counted. In numerous Dox treated cells, the disruption of ΔΨm resulted in the cytosolic accumulation of the marker in monomer form, visualized by a green fluorescence.

The marker aggregated in the undisrupted mitochondria, generating red fluorescence in untreated cells. Quantitative epifluorescence analysis showed a percentage of cells with loss of MMP of 30.0±1.4% compared to the 6.9±1.2%% of cells with no MMP in control cultures (Figure 3A). Flow cytometry analysis supported the conclusion that 24h of Dox treatment induced MMP with an increase in the number of Depsipher green cells (Figure 3B). The loss of ΔΨm was confirmed by a time-course study after 100 µM Dox treatment (Figure 3C). Dox induced loss of MMP within 4h treatment with a statistically significant increase in cells with no MMP (11.4±1.0%) compared to the untreated cells (6.7±0.9%) and about 4-fold more cells with loss of MMP (31.7±14.%) than the control culture (8.4±0.9%) after 24h treatment.

4.2.2. Involvement of Bcl-2 family proteins in Dox-induced apoptosis

From the above results, mitochondria clearly appeared to be involved in Dox-induced toxic effects. The translocation of the proapoptotic protein Bax from the cytosol to the mitochondria is known to be involved in the loss of ΔΨm in numerous models of apoptosis. Nevertheless, Western blot analysis (Figure 4A) and immunofluorescence observations (Figure 4B) showed respectively no change in Bax expression or activation and relocalisation. Moreover, experiments performed on Bax-/- HCT116 cells showed that 100 µM Dox treatment induced both decrease in viability (63.1±1.7%, Figure 4D) and mitochondrial alteration (39.4±2.0%, Figure 4F) which consequently appeared Bax-independent.

On the opposite, the levels of expression of the pro-apoptotic protein Bak and the anti-apoptotic protein Bcl-2 were modified after Dox treatment. Western Blot of Bak protein showed increase in the Bak protein expression (Figure 4A) and Bak-/- HCT116 cells exhibited an increase in viability (88.5±1.8%, Figure 4D), and a decrease in loss of ΔΨm (18.7±1.5%, Figure 4F), in comparison with treated cells (respectively 61.9±1.9% of live cells and 42.2±1.4% of cells with altered mitochondria after 100 µM Dox treatment). The anti-apoptotic factor Bcl-2 seemed also to play a crucial role in Dox-induced apoptosis since a decrease in Bcl-2 protein expression was observed after 8h and 24h of treatment (Figure 4A). Transiently-transfected 16HBE cells (Figure 4C) or stably-transfected HeLa cells with Bcl-2 (Figure 4G-I) were analyzed in regard to viability (Figure 4C, G) and mitochondrial potential (Figure 4C, I). Dox-treated Bcl-2-transfected cells showed an increase in viability and a decrease in percentage of cells with altered mitochondria. In conclusion, the anti-apoptotic protein Bcl-2 and the pro-apoptotic Bak seem to be essential mitochondrial-related factors that regulate Dox-induced apoptosis.

The mitochondrial involvement in Dox-induced apoptosis was verified with HeLa cells stably transfected with viral mitochondria-localized inhibitor of apoptosis (vMIA). In vMIA-stably transfected cells the loss of MMP induced by Dox was reduced (47.6±0.8% for 100 µM Dox vs 4.9±0.8% for vMIA-stably transfected cells) and the percentage of live cells increased (64.9±1.1% for 100 µM Dox vs 86.9±1.0% for vMIA-stably transfected cells), confirming the mitochondrial involvement in Dox-induced apoptotic cell death (Figure 4G and I).

4.3. Dox treatment does not activate the p53 pathway

The study of the p53 protein expression (Figure 4A) that could be observed upstream to Bax-activation, also revealed that Dox-induced toxic effects are p53-independent in the 16HBE cells. This result was confirmed by a transfection experiment followed by viability assay and mitochondrial alteration analysis after Dox treatment (Figure 4C). As demonstrated in Figure 4C, transciently-transfected cells with DN p53 exhibited no increase in the percentage of live cells (63.9±1.3%), in comparison with Neo (64.3±1.3%) or wild-type p53 (65.6±1.8%) transfection. Moreover, no detectable effect of DN p53 on the percentage of cells with altered mitochondria cell was observed (33.4±1.3% for DNp53-transfected cells vs 32.8±1.4% for Neo-transfected cells after 24h of 100 µM Dox treatment), suggesting that p53 was not involved in Dox-induced apoptosis.

4.4. Dox induces specific caspase-dependent cell death

Programmed cell death process is currently driven by the activation of caspases, which are responsible for the specific cleavage of proteins in an ordered manner. We investigated, using EnzChek caspase assay kit, the putative activation of caspase-3 after 30 min and 2 h of treatment by measuring spectrometrically the activity of caspase-3 in cytoplasmic extracts resulting in the cleavage of its substrate. It appeared that within 30 min Dox induced a significant increase in the caspase-3 activity which was time-dependent as the caspase-3 activity increased gradually after 2h and 24h of treatment (11200±650 after 30 min, 16170±660 after 2h and 36560±590 after 24h, in comparison with the control ≤ 7000 for each time of treatment (Arbitrary Units (AU))) (Figure 5A). After 24h treatment we also measured the caspase-8 activity which was not modified in comparison with the control (15370±580 for 100µM Dox-treated cells vs 14620±610 for the control (AU)) (Figure 5B).

The involvement of the different caspases was assessed by measuring the effects of a panel of selective caspase inhibitors added to the culture medium before Dox treatment on the rate of apoptosis (Figure 5C). The induction of apoptosis after 24 hours of treatment with Dox was blocked by the pan-caspase inhibitor z-VAD. Dox-induced apoptosis was also largely prevented by the selective z-DEVD, caspase-3- and z-LEHD, caspase-9-inhibitors (respectively 14.8±2.2% and 17.7±1.5% of apoptosis, reported to the control (100% of apoptosis))

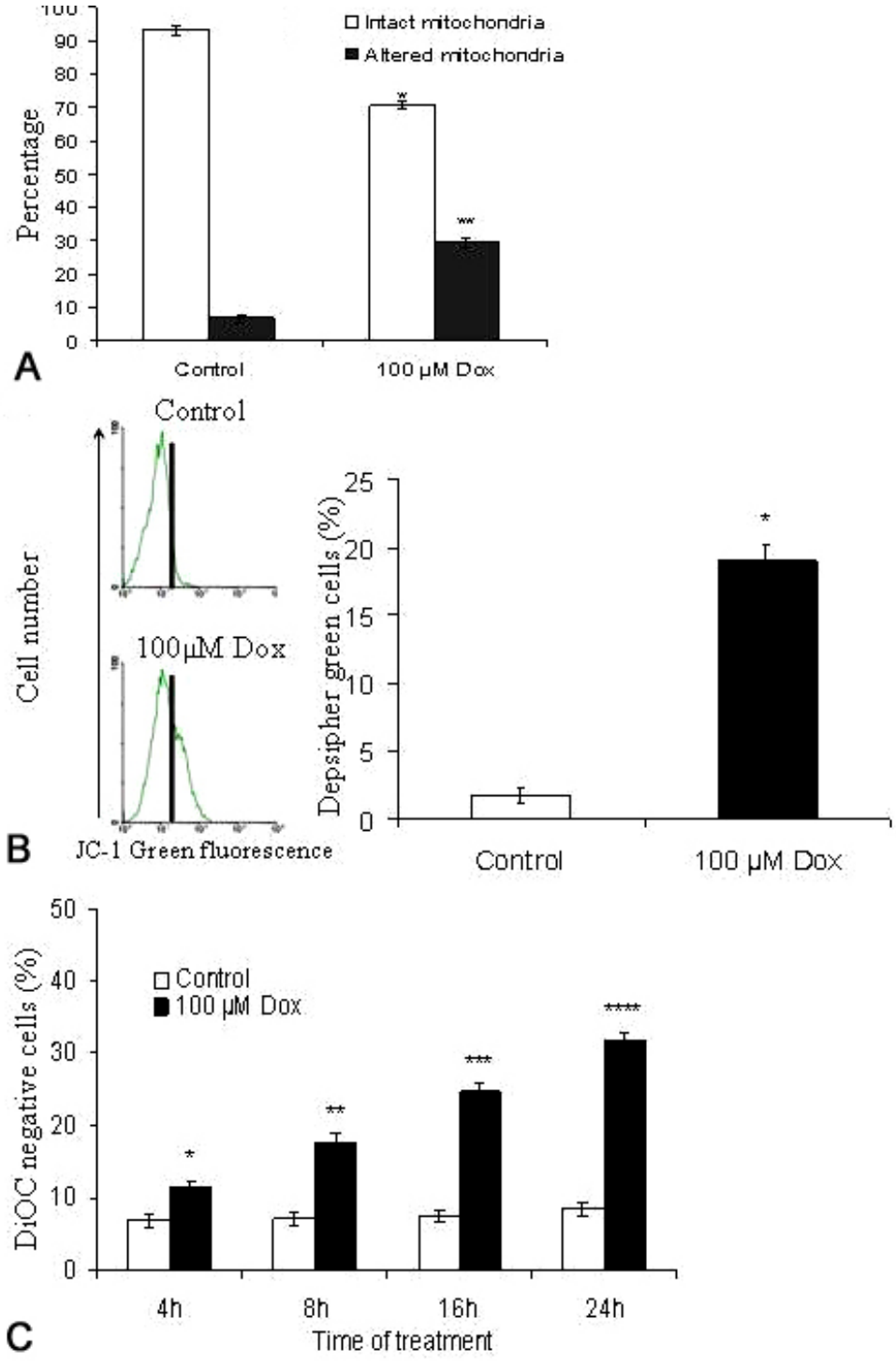

Figure 3. Dox-induced apoptosis triggered mitochondrial alterations. Untreated and treated 16HBE cells were stained with DePsipher dye then (A, B, C). A: Cells were stained with DePsipher dye and cells with intact and altered mitochondria were counted by epifluorescence microscopy after 24h of 100 µM Dox treatment. B: flow cytometric analysis of DePsipher staining after 24h of 100 µM Dox treatment. C: Kinetics of loss of MMP induced by Dox treatment. Data are expressed as percentage of cells with Depsipher green cells for each condition. Data are expressed as percentage of cells with altered mitochondria for each condition. Each bar represents means ± SD of 3 separate determinations. * Values significantly different ($p<0.05$) from control. Among treatment conditions, values not significantly different have the same number of asterisks.

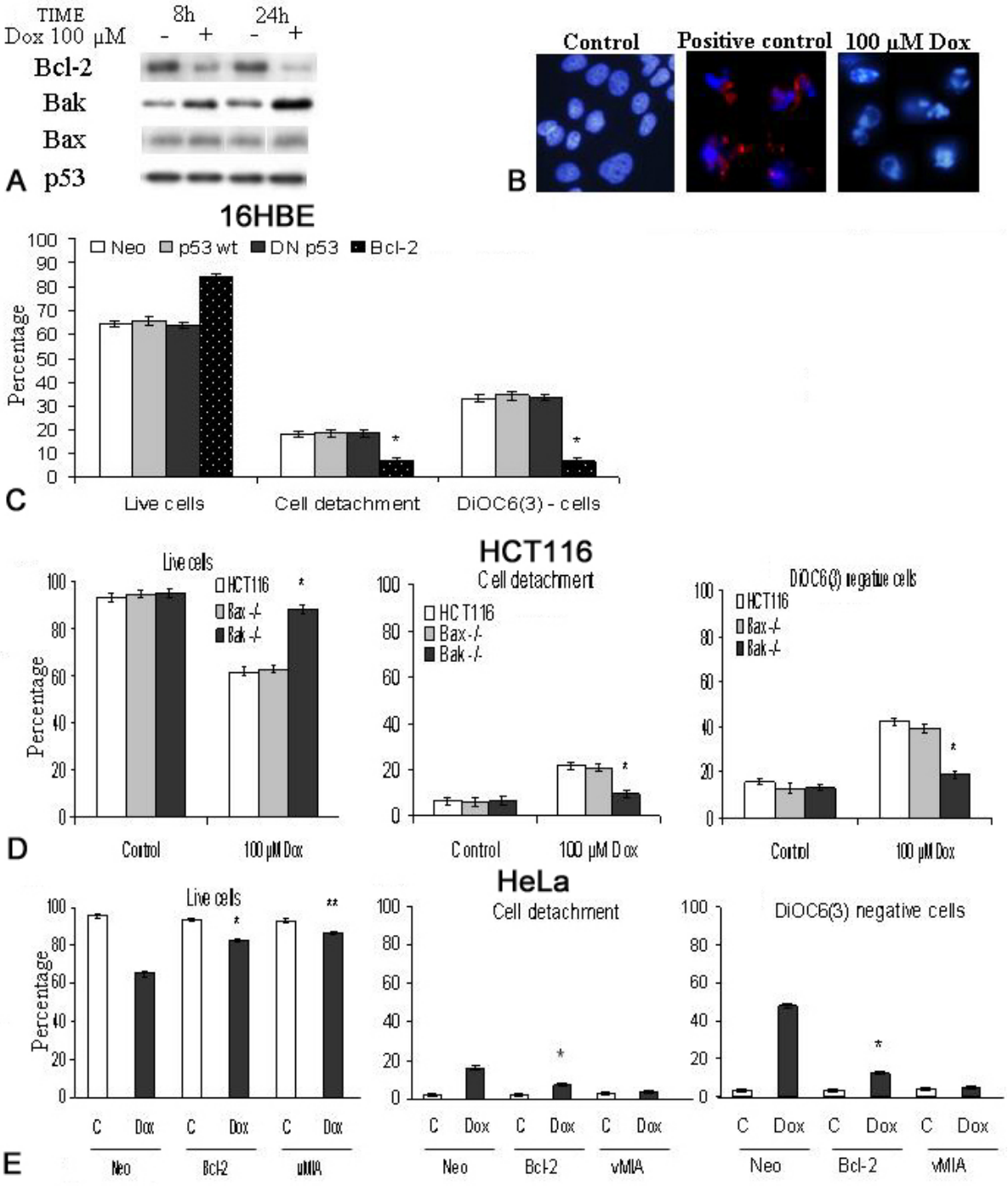

Figure 4. Dox induces apoptosis and cell detachment via Bcl-2 family proteins but not via p53. A: Western blot of p53, Bax, Bak and Bcl-2 in untreated and treated for 8 and 24h with Dox 100 µM. B: Immunodetection of activated Bax in untreated and treated cells with either Dox 100 µM, or HN2 0.1 mM (used as positive control), for 24h. C: 16HBE cells transfected with vectors encoding p53 wt, DN p53 mutant, Bcl-2 or with empty plasmid (Neo) were analyzed after 24h Dox 100 µM treatment. Effects of Dox 100 µM on HCT 116, Bax-/- or Bak-/- cells (D-F)) or on HeLa cells stably transfected with empty (Neo) or Bcl-2 encoding vectors (G-I). Live cells is expressed as the percentage of live cells among the total population assessed by FDA-EtBr, cell detachment is expressed as the percentage of detached cells and mitochondrial depolarization is expressed as the percentage of DiOC6(3) negative cells. Each bar represents means ± SD of 3 separate determinations. * Values significantly different ($p<0.05$) from control. Among treatment conditions, values not significantly different have the same number of asterisks.

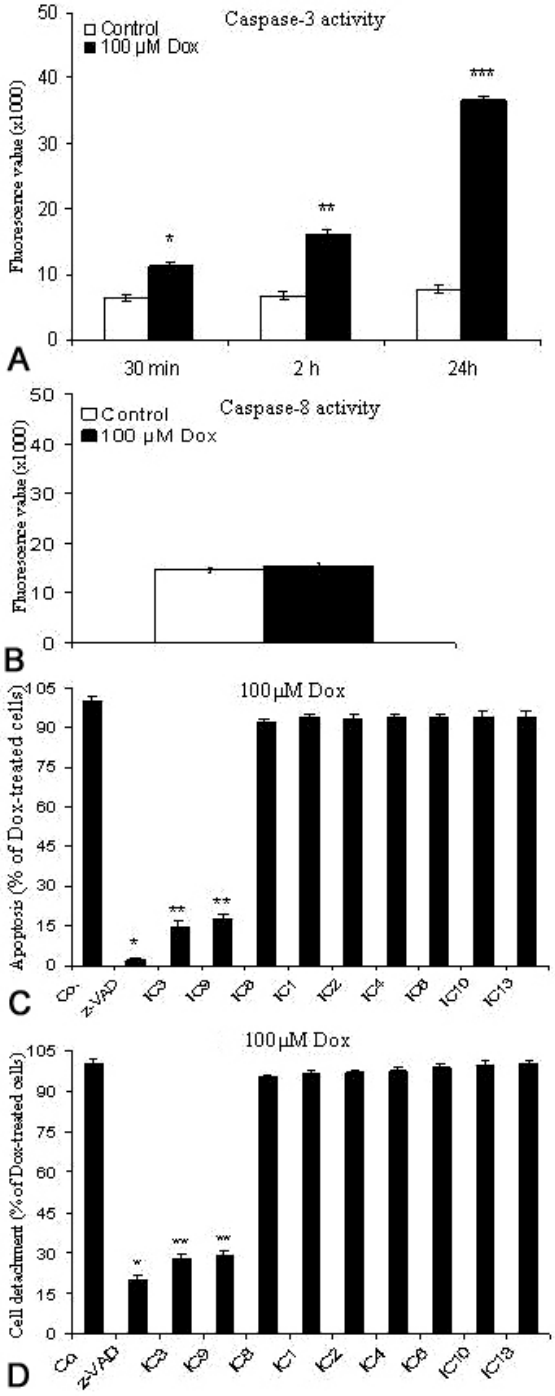

Figure 5. Dox-induced apoptosis and cell detachment are induced by selective caspases. A: activity of caspase-3 was measured in untreated and treated cells for 30min, 2h and 24h with Dox 100 µM. The data are expressed as fluorescence intensity for the cleavage of respective substrate. B: activity of caspase-8 was measured in untreated and treated cells for 24h with Dox 100 µM. The data are expressed as fluorescence intensity for the cleavage of respective substrate. C: Apoptosis rate reported to control cells 24 h after treatment with Dox 100 µM. Cells were pre-incubated 30 min with specific caspase inhibitors, treated with Dox and apoptosis was analysed. D: Cell detachment reported to control cells (100%), 24 h after the beginning of a 100 µM Dox treatment. Cells were pre-incubated 30 min with specific caspase inhibitor, treated with Dox and detached and adherent cells were counted using a hematocytometer. Data are expressed as percentage of cell detachment for the different conditions. Each bar represents means ± SD of 3 separate determinations. * Values significantly different ($p<0.05$) from control. Among treatment conditions, values not significantly different have the same number of asterisks. Legends: ICX means caspase-X inhibitor.

(Figure 5C). The other selective caspase-inhibitors used, inhibitors of caspase-8, z-IETD, caspase-1, z-WEHD, caspase-2 z-VDVAD, caspase-4 z-YVAD, caspase-6 z-VEID, caspase-10 z-AEVD and caspase-13 z-LEED were ineffective. All these results precised the involvement of selective caspases in Dox-induced apoptosis, among which caspase –3 and –9 seem to be the most important.

4.5. Dox-induced apoptosis and cell detachment are related

Dox-induced cell detachment was investigated with respect of the behaviour of the two mitochondrial related proteins Bak and Bcl-2 which were shown to play a key role in Dox-induced apoptosis. Cell detachment was prevented after Dox treatment in 16HBE and HeLa cells both transfected with Bcl-2 (Figure 4C and H), as well as in the Bak-/- HCT116 cells (Figure 4E). Conversely, p53 and Bax which were not involved in Dox-induced apoptosis had no effect on cell detachment (Figure 4C, E). HeLa cells stably transfected with vMIA, able to inibit mitochondrial-related apoptosis, were also protected from Dox-induced cell detachment (Figure 4H). Moreover, caspases involved in Dox-induced execution of apoptosis, caspase-3 and –9, appeared to be also triggered in Dox-induced cell detachment (respectively 28.1±1.5% and 29.0±1.6% of cell detachment, reported to the control (100% of cell detachment)) (Figure 5D).

5. DISCUSSION

In this study, we determined the early mechanisms of toxicity induced by Dox in the 16HBE human bronchial epithelial cell line. We have tested Dox concentrations in the range of 20 to 100 µM. Our experiments showed that Dox induced several various toxic effects, all of them time- and concentration-dependent. This concentration-dependence of toxic effects induced by Dox was also related in others cell lines for a wide range of concentrations. Thus, in the SV-40 transformed human embryonic lung fibroblasts (WI 38 VA 13), a respiratory epithelial-like cell line, the Dox-induced toxicity appeared from concentrations above 0.4 µM (27). Likewise, in various mammalian cell cultures, the toxic concentrations was found to be above 4-10 µM (9).

Our results demonstrated that Dox treatment induced an inhibition of 16HBE proliferation (Figure 1A) as observed *in vitro* in other cells (6, 8, 27-33) or in vivo (12, 34, 35). Therefore, Dox anti-proliferative effect has been investigated in respect with the occurrence of cell cycle arrest, cell detachment or cell death induction. Dox induced an increase in number of S-phase cells correlated with a decrease in the cell number of the phase G1 and G2/M detected by flow cytometry of the cell DNA content (Figure 1C). This increase in S-phase cells could be due to cell cycle arrest within the S phase and subsequent accumulation of S-phase cells (Figure 1D). This result suggested that Dox did not cause any inhibition of G1/S switching and was consistent with the absence of p53 pathway activation after Dox treatment (Figure 4A, C). Thus, dox-induced cell cycle arrest could partly explain the proliferation inhibition observed after Dox treatment. The anti-proliferative effect could also be explained by an increase in cell detachment, since cell detachment was observed within 12h for the highest concentrations and increased up with time of Dox exposure (Figure 2A). Dox-induced cell detachment has also been reported in periodontal ligament derived fibroblasts for concentrations above 50 µM (10). The proliferation inhibition could also be due to cell death process induced by Dox. In agreement with cell cycle arrest in S phase, an event that triggers caspase-dependent apoptotic cell death, Dox clearly induced a substantial increase in the sub-G0/G1 fraction resulting from the DNA cleavage characteristic of the apoptotic process. Nevertheless, complementary experiments demonstrated that apoptosis was not the only type of death induced by Dox. Thus, FDA-EtBr labelling revealed that the decrease in live cell number was essentially correlated with a proportional increase in apoptotic cell number but that cell exposure to high concentrations was followed by an emerging fraction of necrotic cells. This toxicity was also found in human embryonic lung fibroblasts with a complete cell death after 96h exposure with Dox at 200 µM (27).

The faculty to decrease the side effects associated to Dox treatment and/or to "turn on" Dox-induced apoptosis requires a better comprehension of the apoptotic process triggered by Dox. As a key component of the classical apoptotic process, we first have studied the mitochondrial involvement in Dox-induced apoptosis. We have shown that Dox clearly induced signs of MMP such as the dissipation of $\Delta\psi m$ (Figure 3). The involvement of the mitochondria–related proteins Bak (Figure 5A, D-F) and Bcl-2 (Figure 4A, C, G-I) emphasized the key role of mitochondria in Dox-induced apoptosis. The pro-apoptotic protein Bak was up-regulated in Dox treated cells, and the improvement in survival as well as the decrease in loss of MMP of HCT116 Bak-/- cells confirmed the role of Bak in mitochondrial alteration and in viability decrease. The early decrease in the anti-apoptotic protein Bcl-2 expression, as soon as 8h, showed its involvement in Dox-induced apoptosis. Moreover, 16HBE cells transfected with a Bcl-2 encoding vector and experiments carried out on HeLa cells overexpressing Bcl-2 specified its role in mitochondrial alteration, with a decline in loss of mitochondrial potential, and maintain of cell viability. These data are in agreement with previous findings showing that Bcl-2 family proteins play an important role in regulation of apoptosis (36, 37). In spite of the active roles of Bak and Bcl-2, apoptosis induced by Dox seemed to be Bax-independent, as revealed by the absence of adjustment in Bax expression after Dox treatment (Figure 4A) and by similar response of the Bax-/- cell line and non-transfected HCT116 cells regarding loss of mitochondrial potential and viability decrease (Figure 4D, F). Likewise, Dox-induced apoptosis was revealed to be p53-independent as p53 protein expression did not change after Dox treatment (Figure 4A) and as Dox-induced toxic effects did not change in 16HBE cells transiently transfected with wild-type human p53 cDNA or with mutant p53 cDNA (Figure 4C). This p53-independence of Dox-induced apoptosis could be explain by a p53-independent apoptotic process even in presence of DNA damage (38, 39) and could explain the Bax-

independence of Dox-induced apoptosis as it was demonstrated that p53 may represent a key factor in the control of Bax expression (40). In addition, the percentage of apoptotic cells was very close to the percentage of cells with MMP and HeLa cells stably transfected with viral mitochondria-localized inhibitor of apoptosis (vMIA), which prevents MMP (41), sustained the survival of Dox treated cells. Taken together, all these results established the key role of mitochondrial-involvement in Dox-induced apoptosis.

Programmed cell death is also currently driven by the activation of cysteine-proteases named caspases, which are responsible for the specific cleavage of proteins in an ordered manner. Our data demonstrated that Dox-induced apoptosis is caspase-dependent, since the induction of apoptosis by a 24 hours Dox treatment was blocked by the pan-caspase inhibitor z-VAD added to the culture medium before Dox treatment (Figure 5C). We investigated the activity of two caspases, the caspase-3 (Figure 5A), final executioner of apoptotic pathway and the caspase-8 (Figure 5B), involved in Death Receptor mediated apoptosis. It clearly appeared that Dox induced an early activation of caspase-3, as soon as 30 min, increasing up with time. Nevertheless, the caspase-8 activity was not modified suggesting that Dox-induced apoptotic pathway seemed not related to the death receptor pathway. This was confirmed with a panel of selective caspase inhibitors (Figure 5C). The only caspase-inhibitors being effective are the caspase-3 and -9 inhibitors. This underlined the caspase-dependence of Dox-induced apoptosis closely related to the mitochondrial apoptotic pathway (42, 43).

These results demonstrated that Dox-induced apoptosis involved the mitochondrial-related proteins Bcl-2 and Bak and the caspase-3 and -9 activation, but was p53- and caspase-8-independent. Thus, we can conclude that Dox triggers an apoptosis mediated by mitochondrial-pathway.

Afterwards, we sought the involvement of mitochondrion and caspases, evidenced as key components of the Dox-induced apoptotic pathway, in cell detachment. The two mitochondrial related proteins Bak and Bcl-2 involved in apoptotic response also showed a significant effect on cell detachment. Transient transfection with Bcl-2 gene abrogated cell detachment and HeLa cells stably transfected with vMIA, inhibiting mitochondrial-related apoptosis, were protected from cell detachement. These results showed the mitochondrial-involvement in cell detachment. Then, the caspase-dependence of Dox-induced cell detachment was evaluated by measuring the effect of specific caspase-inhibitors on cell detachment. The pan-caspase inhibitor z-VAD inhibited Dox-induced cell detachment. The two caspases involved in cell detachment seem to be the final executioner caspase-3 and the mitochondrial-related caspase-9. These results indicated the caspase-involvement in cell detachment. Therefore, all these elements suggest that Dox-induced apoptotic execution and cell detachment are closely associated (44-46). During Dox treatment, Bcl-2 decreased expression and loss of MMP, as well as the increase in caspase-3 activity, constituted early events that occurred before the beginning of cell detachment, suggesting that apoptosis could be responsible of cell detachment.

In conclusion, we have shown in this study that Dox treatment generated concomitant toxic effects: cell proliferation inhibition, with cell cycle arrest, apoptosis and cell detachment. Its ability to induce cell proliferation inhibition and apoptosis could represent a major addition to the treatment options available for the management of cancers, and more specifically to the therapeutic management of tumoral cells resistant to death receptor-mediated cell death, as our understanding of the pathways involved in the toxic effects induced by Dox points to the mitochondrion as a central regulator of apoptosis. To activate Dox-induced apoptosis in such cells could allow to restrain their proliferative potential. Nevertheless, further studies have to be carried out to better understand the cell detachment triggered by Dox-induced apoptosis, which could induce a negative synergistic effect during the treatment of metastatic cells.

6. ACKNOWLEDGMENTS

We acknowledge Dr. D.C. Gruenert for providing us with the human bronchial epithelial cell line and the excellent technical assistance of Marie-Claude Gendron for carrying out cytometric experiments. Catherine Brenner is supported by the Association pour la Recherche sur le Cancer (ARC). This work was support by the Délégation Générale pour l'Armement (D.G.A/D.S.P N°95-151).

7. REFERENCES

1. Frucht-Pery, J., E. Sagi, I. Hemo & P. Ever-Hadani: Efficacy of doxycycline and tetracycline in ocular rosacea. *Am J Ophthalmol* 116(1), 88-92 (1993)

2. Solomon, A., M. Rosenblatt, D.Q. Li, Z. Liu, D. Monroy, Z. Ji, B.L. Lokeshwar & S.C. Pflugfelder: Dox inhibition of interleukin-1 in the corneal epithelium. *Invest Ophthalmol Vis Sci* 41(9), 2544-57 (2000)

3. Baxter, B.T., W.H. Pearce, E.A. Waltke, F.N. Littooy, J.W.Jr. Hallett, K.C. Kent, G.R.Jr. Upchurch, E.L. Chaikof, J.L. Mills, B. Fleckten, G.M. Longo, J.K. Lee & R.W. Thompson : Prolonged administration of doxycycline in patients with small asymptomatic abdominal aortic aneurysms: report of a prospective (Phase II) multicenter study. *J Vasc Surg* 36(1), 1-12 (2002)

4. Uitto, V.J., J.D. Firth, L. Nip & L.M. Golub: Doxycycline and chemically modified tetracyclines inhibit gelatinase A (MMP-2) gene expression in human skin keratinocytes. *Ann N Y Acad Sci* 732,140-51 (1994)

5. Bettany, J.T. & R.G. Wolowacz: Tetracycline derivatives induce apoptosis selectively in cultured monocytes and macrophages but not in mesenchymal cells. *Adv Dent Res* 12(2), 136-43 (1998)

6. Liu, J., W. Xiong, L. Baca-Regen, H. Nagase & B.T. Baxter: Mechanism of inhibition of matrix metalloproteinase-2 expression by Dox in human aortic smooth muscle cells. *J Vasc Surg* 38(6), 1376-83 (2003)

7. Fife, R.S., G.W.Jr. Sledge, B.J. Roth & C. Proctor: Effects of Dox on human prostate cancer cells in vitro. *Cancer Lett* 127(1-2), 37-41 (1998)

8. Van den Bogert, C., B.H. Dontje, M. Holtrop, T.E. Melis, J.C. Romijn, J.W. Van Dongen & A.M. Kroon: Arrest of the proliferation of renal and prostate carcinomas of human origin by inhibition of mitochondrial protein synthesis. *Cancer Res* 46(7), 3283-9 (1986a)

9. Hovel, H. & K.H. Frieling: The use of Dox, mezlocillin and clotrimazole in cell culture media as contamination prophylaxis. *Dev Biol Stand* 66, 23-8 (1987)

10. Tsukuda, N. & W.L. Gabler: The influence of Dox of the attachment of fibroblasts to gelatin-coated surfaces and its cytotoxicity. *J Periodontol* 64(12), 1219-24 (1993)

11. Izumi, M. & D.M. Gilbert: Homogeneous tetracycline-regulatable gene expression in mammalian fibroblasts. *J Cell Biochem* 76(2), 280-9 (1999)

12. Prall, A.K., G.M. Longo, W.G. Mayhan, E.A. Waltke, B. Fleckten, R.W. Thompson & B.T. Baxter: Dox in patients with abdominal aortic aneurysms and in mice: comparison of serum levels and effect on aneurysm growth in mice. *J Vasc Surg* 35(5), 923-9 (2002)

13. Fife, R.S., B.T. Rougraff, C. Proctor & G.W.Jr. Sledge: Inhibition of proliferation and induction of apoptosis by Dox in cultured human osteosarcoma cells. *J Lab Clin Med* 130(5), 530-4 (1997)

14. Luo, X., I. Budihardjo, H. Zou, C. Slaughter, & X. Wang: Bid, a Bcl2 interacting protein, mediates cytochrome c release from mitochondria in response to activation of cell surface death receptors. *Cell* 94(4), 481-90 (1998)

15. Goldstein, J.C., N.J. Waterhouse, P. Juin, G.I. Evan & D.R. Green: The coordinate release of cytochrome c during apoptosis is rapid, complete and kinetically invariant. *Nat Cell Biol* 2(3), 156-62 (2000)

16. Marzo I., C. Brenner, N. Zamzami, S.A. Susin, G. Beutner, D. Brdiczka, R. Remy, Z.H. Xie, J.C. Reed & G. Kroemer: The permeability transition pore complex: a target for apoptosis regulation by caspases and bcl-2-related proteins. *J Exp Med* 187(8), 1261-71 (1998)

17. Green, D.R. & G. Kroemer: The pathophysiology of mitochondrial cell death. *Science* 305(5684), 626-9 (2004)

18. Cunha, B.A: The chlamydial pneumonias. *Drugs Today (Barc)* 34(12), 1005-12 (1998)

19. Jernigan, J.A., D.S. Stephens, D.A. Ashford, C. Omenaca, M.S. Topiel, M. Galbraith, M. Tapper, T.L. Fisk, S. Zaki, T. Popovic, R.F. Meyer, C.P. Quinn, S.A. Harper, S.K. Fridkin, J.J. Sejvar, C.W. Shepard, M. McConnell, J. Guarner, W.J. Shieh, J.M. Malecki, J.L. Gerberding, J.M. Hughes & B.A. Perkins: Anthrax Bioterrorism Investigation Team. Bioterrorism-related inhalational anthrax: The first 10 cases reported in the United-States. *Emerging Infectious Diseases* 7, 933-944 (2001)

20. Mayer, T.A., S. Bersoff-Matcha, C. Murphy, J. Earls, S. Harper, D. Pauze, M. Nguyen, J. Rosenthal, D.Jr. Cerva, G. Druckenbrod, D. Hanfling, N. Fatteh, A. Napoli, A. Nayyar & E.L. Berman: Clinical presentation of inhalation anthrax following bioterrorism exposure. Report of 2 surviving patients. *JAMA* 286, 2549-53 (2001)

21. Guignabert C., L. Taysse, J.H. Calvet, E. Planus, S. Delamanche, S. Galiacy & M.P. d'Ortho: Effect of doxycycline on sulfur mustard-induced respiratory lesions in guinea pigs. *Am J Physiol Lung Cell Mol Physiol* 289(1), 67-74 (2005)

22. Boisvieux-Ulrich, E., M. Sourdeval & F. Marano : CD437, a synthetic retinoid, induces apoptosis in human respiratory epithelial cells via caspase-independent mitochondrial and caspase-8-dependent pathways both up-regulated by JNK signaling pathway. *Exp Cell Res* 307(1), 76-90 (2005)

23. Cozens, A.L., M.J. Yezzi, K. Kunzelmann, T. Ohrui, L. Chin, K. Eng, W.E. Finkbeiner, J.H. Widdicombe & D.C. Gruenert: CFTR expression and chloride secretion in polarized immortal human bronchial epithelial cells. *Am J Respir Cell Mol Biol* 10(1), 38-47 (1994)

24. Lemaire, C., K. Andreau, V. Souvannavong & A. Adam: Inhibition of caspase activity induces a switch from apoptosis to necrosis. *FEBS Lett* 425(2), 266-70 (1998)

25. Zamzami N., P. Marchetti, M. Castedo, C. Zanin, J.L. Vayssiere, P.X. Petit & G. Kroemer: Reduction in mitochondrial potential constitutes an early irreversible step of programmed lymphocyte death in vivo. *J Exp Med* 181(5), 1661-72 (1995)

26. Ilic D., E.A. Almeida, D.D. Schlaepfer, P. Dazin, S. Aizawa & C.H. Damsky. Extracellular matrix survival signals transduced by focal adhesion kinase suppress p53-mediated apoptosis. *J Cell Biol* 143: 547-560 (1998)

27. Ermak, G., V.J. Cancasci & K.J. Davies: Cytotoxic effect of Dox and its implications for tet-on gene expression systems. *Anal Biochem* 318(1), 152-4 (2003)

28. Van den Bogert, C., G. Van Kernebeek, L. de Leij & A.M. Kroon: Inhibition of mitochondrial protein synthesis leads to proliferation arrest in the G1-phase of the cell cycle. *Cancer Lett* 32(1), 41-51 (1986b)

29. Duivenvoorden, W.C., H.W. Hirte & G. Singh: Use of tetracycline as an inhibitor of matrix metalloproteinase

activity secreted by human bone-metastasizing cancer cells. *Invasion Metastasis* 17(6), 312-22 (1997)

30. Liu, J., C.A. Kuszynski & B.T. Baxter: Doxycycline induces Fas/Fas ligand-mediated apoptosis in Jurkat T lymphocytes. *Biochem Biophys Res Commun* 260(2), 562-7 (1999)

31. Tolomeo, M., S. Grimaudo, S. Milano, M. La Rosa, V. Ferlazzo, G. Di Bella, C. Barbera, D. Simoni, P. D'Agostino & E. Cillari: Effects of chemically modified tetracyclines (CMTs) in sensitive, multidrug resistant and apoptosis resistant leukaemia cell lines. *Br J Pharmacol* 133(2), 306-14 (2001)

32. Duivenvoorden, W.C., S.V. Popovic, S. Lhotak, E. Seidlitz, H.W. Hirte, R.G. Tozer & G. Singh: Dox decreases tumor burden in a bone metastasis model of human breast cancer. *Cancer Res* 62(6), 1588-91 (2002)

33. Iwasaki, H., H. Inoue, Y. Mitsuke, A. Badran, S. Ikegaya & T. Ueda: Dox induces apoptosis by way of caspase-3 activation with inhibition of matrix metalloproteinase in human T-lymphoblastic leukemia CCRF-CEM cells. *J Lab Clin Med* 140(6), 382-6 (2002)

34. Petrinec, D., S. Liao, D.R. Holmes, J.M. Reilly, W.C. Parks & R.W. Thompson: Dox inhibition of aneurysmal degeneration in an elastase-induced rat model of abdominal aortic aneurysm: preservation of aortic elastin associated with suppressed production of 92 kD gelatinase. *J Vasc Surg* 23(2), 336-46 (1996)

35. Boyle, J.R., E. McDermott, M. Crowther, A.D. Wills, P.R. Bell & M.M. Thompson: Dox inhibits elastin degradation and reduces metalloproteinase activity in a model of aneurysmal disease. *J Vasc Surg* 27(2), 354-61 (1998)

36. Kim, R., M. Emi & K. Tanabe: Role of mitochondria as the gardens of cell death. *Cancer Chemother Pharmacol* 21, 1-9 (2005)

37. Lucken-Ardjomande, S & J.C. Martinou: Regulation of Bcl-2 proteins and of the permeability of the outer mitochondrial membrane. *C R Biol* 328(7), 616-31 (2005)

38. Kaina, B: DNA damage-triggered apoptosis: critical role of DNA repair, double-strand breaks, cell proliferation and signalling. *Biochemical Pharmacology* 66, 1547–1554 (2003)

39. Norbury, C.J. & B. Zhivotovsky: DNA damage-induced apoptosis. *Oncogene* 23, 2797–2808 (2004)

40. Thornborrow E.C., S. Patel, A.E. Mastropietro, E.M. Schwartzfarb & J.J. Manfredi: A conserved intronic response element mediates direct p53-dependent transcriptional activation of both the human and murine bax genes. *Oncogene* 7, 990–999 (2002)

41. Boya, P., A.L. Pauleau, D. Poncet, R.A. Gonzalez-Polo, N. Zamzami & G. Kroemer: Viral proteins targeting mitochondria: controlling cell death. *Biochim Biophys Acta* 1659(2-3), 178-89 (2004)

42. Breckenridge, D.G. & D. Xue: Regulation of mitochondrial membrane permeabilization by BCL-2 family proteins and caspases. *Curr Opin Cell Biol* 16(6), 647-52 (2004)

43. Green, D.R: Apoptotic pathways: ten minutes to dead. *Cell* 121(5), 671-4 (2005)

44. Grossmann, J., K. Walther, M. Artinger, S. Kiessling & J. Scholmerich: Apoptotic signaling during initiation of detachment-induced apoptosis ("anoikis") of primary human intestinal epithelial cells. *Cell Growth Differ* 12(3), 147-55 (2001)

45. Chay, K.O., S.S. Park & J.F. Mushinski: Linkage of caspase-mediated degradation of paxillin to apoptosis in Ba/F3 murine pro-B lymphocytes. *J Biol Chem* 277(17), 14521-9 (2002)

46. Grossmann, J: Molecular mechanisms of "detachment-induced apoptosis-anoikis. *Apoptosis* 7, 247-60 (2002)

Key Words: Epithelium, Airway, Respiratory tract, Doxycycline, Apoptosis, Necrosis, Mitochondrion, Bcl-2, Caspase-3, Caspase-9

Send correspondence to: Dr Matthieu Sourdeval, Laboratoire de Cytophysiologie et Toxicologie Cellulaire, Université Paris7, Denis Diderot, case 70-73, 2 place Jussieu, 75251 Paris Cedex 05, France. Tel: 33144276062, Fax: 33144276999, E-mail: msourdeval@paris7.jussieu.fr

http://www.bioscience.org/current/vol11.htm